TECHNISCHE UNIVERSITÄT
KAISERSLAUTERN

A Second Order Non-smooth Variational Model for Restoring Manifold-valued Images

Ronny Bergmann*

Department of Mathematics, University of Kaiserslautern

May 23, 2016

SIAM Converence on Imaging Science
MS1: Inversion of Non-linear Image Formation Models Pt. I,

Albuquerque, NM, USA.

FELIX KLEIN
ZENTRUM FÜR
MATHEMATIK

funded by
DAAD
DFG

*joint work with M. Bačák (MPI MIS Leipzig), J. Persch, G. Steidl (U Kaiserslautern),
A. Weinmann (H Darmstadt)

Contents

Restoring Images: Denoising and Inpainting

Introducing discrete total variation models for real valued data.

- given noisy image $f\colon \mathcal{V} \to \mathbb{R}$, $\mathcal{V} \subseteq \mathcal{G} = \{1,\dots,N\} \times \{1,\dots,M\}$
- reconstruct original image $u_0 : \mathcal{G} \to \mathbb{R}$
- pixel from $\mathcal{G}\backslash\mathcal{V}$ have to be inpainted
- approach: Minimize variational model

$$\mathcal{E}(u) := \underbrace{F(f,u)}_{\text{data term}} + \underbrace{\alpha\, R(u)}_{\text{regularization term}}, \qquad \alpha > 0$$

- first order models (total variation, TV) [Rudin, Osher, Fatemi, 1992]
  - isotropic model with discrete gradient $|\nabla u|$: $R_{\text{iso}}(u) := \sum_{i,j} |\nabla u|$
  - anisotropic model: $R_{\text{aniso}}(u) := \sum_{i,j} \left(|u_{i+1,j} - u_{i,j}| + |u_{i,j+1} - u_{i,j}| \right)$
  - edge preserving
- several higher order variational models avoid stair casing effect

[Chambolle, Lions, 1997; Setzer, Steidl, 2008; Bredies, Kunisch, Pock, 2010; Papafitsoros, Schönlieb, 2014]

Restoring Images with Values in Riemannian Manifolds

Here:
Images with pixel values in a Riemannian manifold $\mathcal{M}$

Goal: A Second Order Model for images $f\colon \mathcal{V} \to \mathcal{M}$

Applications with manifold-valued images are for example

- $\mathbb{S}^1$ InSAR, HSI(HSV) color space, phase space
- $\mathbb{S}^2$ directions, chromaticity-brightness colorspace
- $\mathrm{SO}(3)$ orientations, electron backscattered diffraction
- $\mathcal{P}(s)$ DT-MRI, covariance matrices

Riemannian Manifolds

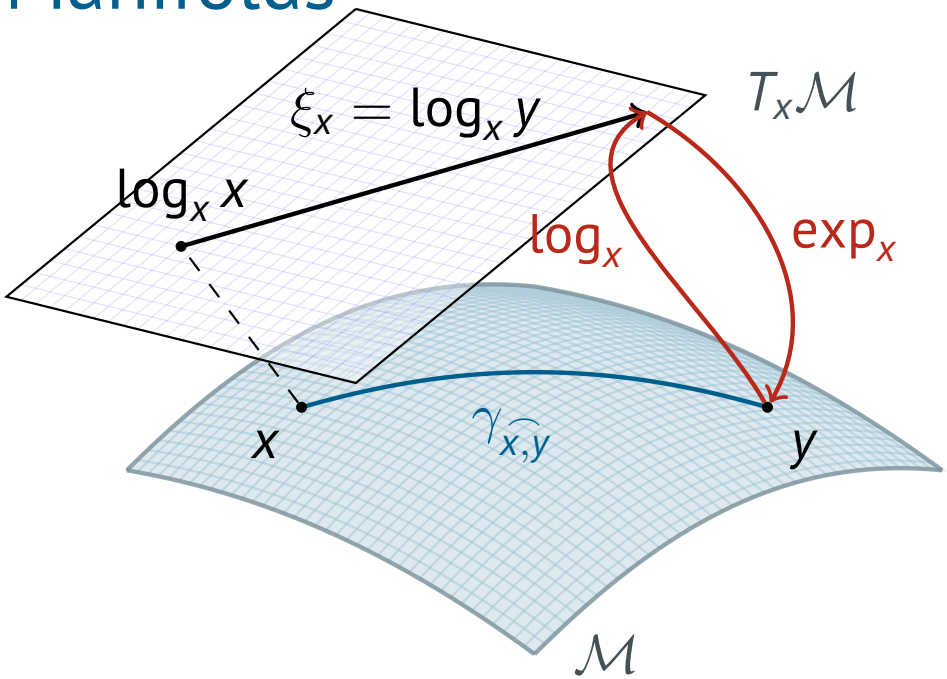

A d-dimensional manifold can be informally defined as a set $\mathcal{M}$ covered with a "suitable" collection of charts, that identify subsets of $\mathcal{M}$ with open subsets of $\mathbb{R}^d$.

[Absil, Mahony, Sepulchre, 2008]

geodesic $\gamma_{\widehat{x,y}}$ shortest path (on $\mathcal{M}$) connecting $x, y \in \mathcal{M}$.

tangential plane $T_x\mathcal{M}$ at x

logarithmic map $\log_x y = \dot{\gamma}_{\widehat{x,y}}(0)$, "velocity towards y"

exponential map $\exp_x \xi_x = \gamma(1)$ of geodesic γ with $\gamma(0) = x$, $\dot{\gamma}(0) = \xi_x$

Symmetric Positive Definite Matrices A, $x^{\mathrm{T}}Ax > 0$

$\mathcal{P}(3)$: each pixel is a 3×3 symmetric positive definite matrix or an ellipsoid

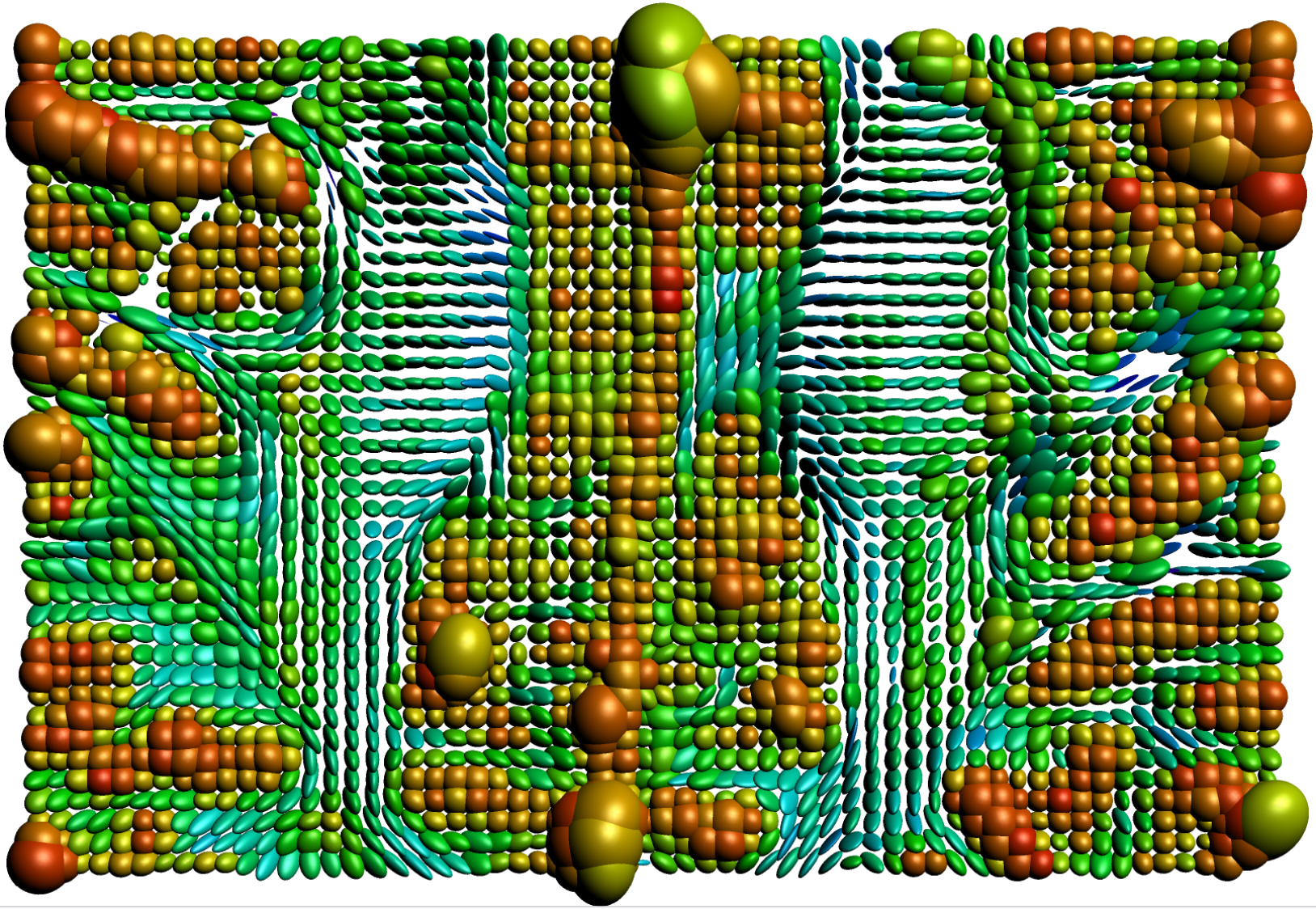

First and Second Order Differences

Let's restrict ourselves to signals for now...

$\mathcal{G} = \{1, \dots, N\}, \mathcal{V} \subset \mathcal{G}$

On $\mathbb{R}^n$

- line $\gamma(t) = x + t(y - x)$
- distance $\|x - y\|_2$
- first order model

$$\sum_{i \in \mathcal{V}} \|f_i - u_i\|_2^2 + \alpha \sum_{i \in \mathcal{G} \setminus \{N\}} \|u_i - u_{i+1}\|_2$$

Riemannian manifold $\mathcal{M}$

- geodesic path $\gamma_{\widehat{x,y}}(t)$
- geodesic distance $d\colon \mathcal{M} \times \mathcal{M} \to \mathbb{R}_{\geq 0}$
- first order model

[Strekalovskiy, Cremers, 2011; Lellmann et al., 2013; Weinmann et. al., 2014]

$$\sum_{i \in \mathcal{V}} d(f_i, u_i)^2 + \alpha \sum_{i \in \mathcal{G} \setminus \{N\}} d(u_i, u_{i+1})$$

First and Second Order Differences

Let's restrict ourselves to signals for now...

$\mathcal{G} = \{1, \dots, N\}$, $\mathcal{V} \subset \mathcal{G}$

On $\mathbb{R}^n$

- line $\gamma(t) = x + t(y - x)$
- distance $\|x - y\|_2$
- first order model

$$\sum_{i \in \mathcal{V}} \|f_i - u_i\|_2^2 + \alpha \sum_{i \in \mathcal{G} \setminus \{N\}} \|u_i - u_{i+1}\|_2$$

- second oder difference

$$\|x - 2y + z\|_2$$

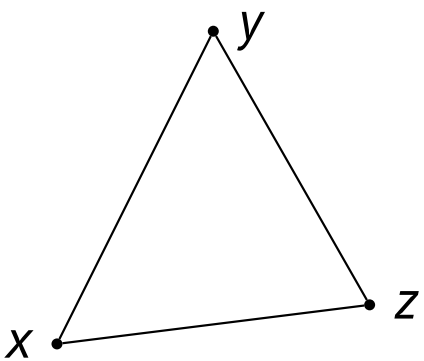

Riemannian manifold $\mathcal{M}$

- geodesic path $\gamma_{\overset{\frown}{x,y}}(t)$
- geodesic distance $d\colon \mathcal{M} \times \mathcal{M} \to \mathbb{R}_{\geq 0}$
- first order model

[Strekalovskiy, Cremers, 2011; Lellmann et al., 2013; Weinmann et. al., 2014]

$$\sum_{i \in \mathcal{V}} d(f_i, u_i)^2 + \alpha \sum_{i \in \mathcal{G} \setminus \{N\}} d(u_i, u_{i+1})$$

- How to model that on $\mathcal{M}$?

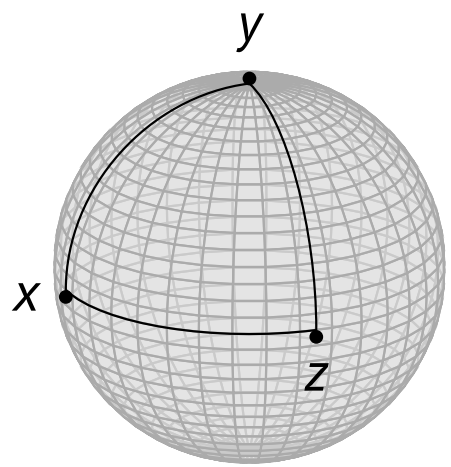

$\mathcal{M} = \mathbb{S}^2$

First and Second Order Differences

Let's restrict ourselves to signals for now...

$\mathcal{G} = \{1, \dots, N\}, \mathcal{V} \subset \mathcal{G}$

On $\mathbb{R}^n$

- line $\gamma(t) = x + t(y - x)$
- distance $\|x - y\|_2$
- first order model

$$\sum_{i \in \mathcal{V}} \|f_i - u_i\|_2^2 + \alpha \sum_{i \in \mathcal{G} \setminus \{N\}} \|u_i - u_{i+1}\|_2$$

- second oder difference

$$2\|\tfrac{1}{2}(x + z) - y\|_2$$

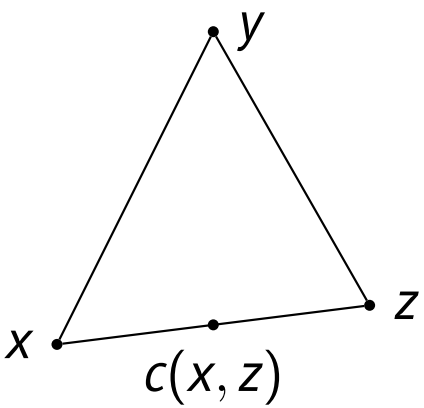

Riemannian manifold $\mathcal{M}$

- geodesic path $\gamma_{\overset{\frown}{x,y}}(t)$
- geodesic distance $d\colon \mathcal{M} \times \mathcal{M} \to \mathbb{R}_{\geq 0}$
- first order model

[Strekalovskiy, Cremers, 2011; Lellmann et al., 2013; Weinmann et. al., 2014]

$$\sum_{i \in \mathcal{V}} d(f_i, u_i)^2 + \alpha \sum_{i \in \mathcal{G} \setminus \{N\}} d(u_i, u_{i+1})$$

- idea: mid point formulation

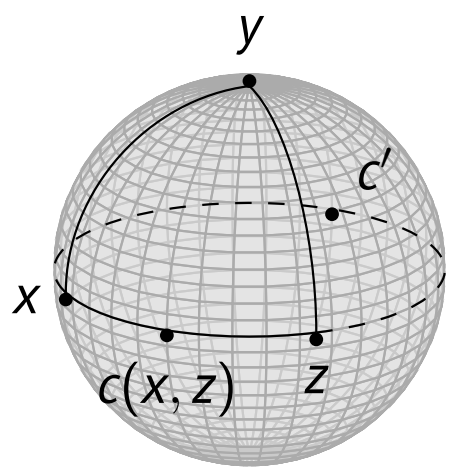

$\mathcal{M} = \mathbb{S}^2$

First and Second Order Differences

Let's restrict ourselves to signals for now...

$\mathcal{G} = \{1, \dots, N\}, \mathcal{V} \subset \mathcal{G}$

On $\mathbb{R}^n$

- line $\gamma(t) = x + t(y - x)$
- distance $\|x - y\|_2$
- first order model

$$\sum_{i \in \mathcal{V}} \|f_i - u_i\|_2^2 + \alpha \sum_{i \in \mathcal{G} \setminus \{N\}} \|u_i - u_{i+1}\|_2$$

- second oder difference

$2\|c(x,z) - y\|_2$, $c(x,y)$: mid point

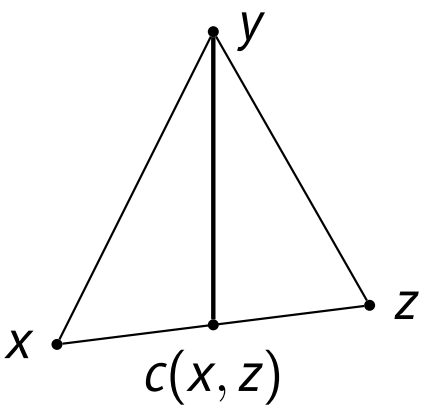

Riemannian manifold $\mathcal{M}$

- geodesic path $\gamma_{\widehat{x,y}}(t)$
- geodesic distance $d\colon \mathcal{M} \times \mathcal{M} \to \mathbb{R}_{\geq 0}$
- first order model

[Strekalovskiy, Cremers, 2011; Lellmann et al., 2013; Weinmann et. al., 2014]

$$\sum_{i \in \mathcal{V}} d(f_i, u_i)^2 + \alpha \sum_{i \in \mathcal{G} \setminus \{N\}} d(u_i, u_{i+1})$$

- idea: mid point formulation

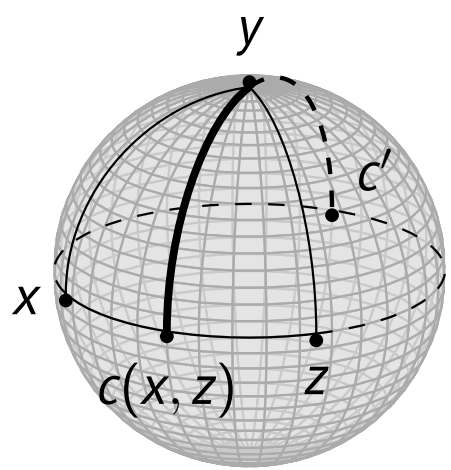

$\mathcal{M} = \mathbb{S}^2$

A Second Order TV-type Model

Mid points between $x, z \in \mathcal{M}$:

$$\mathcal{C}_{x,z} := \left\{ c \in \mathcal{M} : c = \gamma_{\widehat{x,z}}\left(\tfrac{T}{2}\right) \text{ for any geodesic } \gamma_{\widehat{x,z}},\quad T := \mathcal{L}(\gamma_{\widehat{x,z}}) \right\}$$

The Absolute Second Order Difference:

$$d_2(x,y,z) := \min_{c \in \mathcal{C}_{x,z}} d(c,y), \qquad x,y,z \in \mathcal{M}.$$

$\Rightarrow$ Second Order TV-type Model for $\mathcal{M}$-valued signals f

$$\mathcal{E}(u) := \sum_{i \in \mathcal{V}} d(f_i, u_i)^2 + \alpha \sum_{i \in \mathcal{G}\setminus\{N\}} d(u_i, u_{i+1}) + \beta \sum_{i \in \mathcal{G}\setminus\{1,N\}} d_2(u_{i-1}, u_i, u_{i+1})$$

A Second Order TV-type Model

Mid points between $x, z \in \mathcal{M}$:

$$\mathcal{C}_{x,z} := \left\{ c \in \mathcal{M} : c = \gamma_{\widehat{x,z}}\left(\tfrac{T}{2}\right) \text{ for any geodesic } \gamma_{\widehat{x,z}},\quad T := \mathcal{L}(\gamma_{\widehat{x,z}}) \right\}$$

The Absolute Second Order Difference:

$$d_2(x,y,z) := \min_{c \in \mathcal{C}_{x,z}} d(c,y), \qquad x,y,z \in \mathcal{M}.$$

$\Rightarrow$ Second Order TV-type Model for $\mathcal{M}$-valued signals f

$$\mathcal{E}(u) := \sum_{i \in \mathcal{V}} d(f_i, u_i)^2 + \alpha \sum_{i \in \mathcal{G}\setminus\{N\}} d(u_i, u_{i+1}) + \beta \sum_{i \in \mathcal{G}\setminus\{1,N\}} d_2(u_{i-1}, u_i, u_{i+1})$$

For images additionally: use $\|w - x + y - z\|_2 = 2\|\frac{1}{2}(w+y) - \frac{1}{2}(x+z)\|_2$ for Absolute Second Order Mixed Difference

$$d_{1,1}(w,x,y,z) := \min_{c \in \mathcal{C}_{w,y}, \tilde{c} \in \mathcal{C}_{x,z}} d(c,\tilde{c}), \qquad w,x,y,z \in \mathcal{M}.$$

Proximal Mappings and the CPPA

How to minimize the Second Order TV-type Model on $\mathcal{M}$?

To compute a minimizer of $\mathcal{E}(u)$: proximal mappings

For a function $\varphi\colon \mathcal{M}^n \to (-\infty, +\infty]$ and $\lambda > 0$ the proximal mapping is defined by

[Moreau, 1965; Rockafellar, 1976; Ferreira, Oliveira, 2002]

$$\operatorname{prox}_{\lambda\varphi}(g) := \operatorname*{arg\,min}_{u\in\mathcal{M}^n} \frac{1}{2}\sum_{i=1}^{n} d(u_i, g_i)^2 + \lambda\varphi(u).$$

Note: For a minimizer u^* of φ it holds $\operatorname{prox}_{\lambda\varphi}(u^*) = u^*$.

Proximal Mappings and the CPPA

How to minimize the Second Order TV-type Model on $\mathcal{M}$?

To compute a minimizer of $\mathcal{E}(u)$: proximal mappings

For a function $\varphi\colon \mathcal{M}^n \to (-\infty, +\infty]$ and $\lambda > 0$ the proximal mapping is defined by [Moreau, 1965; Rockafellar, 1976; Ferreira, Oliveira, 2002]

$$\operatorname{prox}_{\lambda\varphi}(g) := \operatorname*{arg\,min}_{u\in\mathcal{M}^n} \frac{1}{2}\sum_{i=1}^{n} d(u_i, g_i)^2 + \lambda\varphi(u).$$

Note: For a minimizer u^* of φ it holds $\operatorname{prox}_{\lambda\varphi}(u^*) = u^*$.

For $\varphi = \sum_{l=1}^{c} \varphi_l$ use Cyclic Proximal Point Algorithm (CPPA) [Bertsekas, 2011; Bačák, 2014]

$$x^{(k+\frac{l+1}{c})} = \operatorname{prox}_{\lambda_k\varphi_l}(x^{(k+\frac{l}{c})}), \quad i = 0, \dots, c-1,\ k > 0$$

For real-valued data: Converges to a minimizer if $\{\lambda_k\}_{k\in\mathbb{N}} \in \ell_2(\mathbb{Z})\backslash\ell_1(\mathbb{Z})$.

Minimizing the Second Order Model

Applying the CPPA to our model on manifolds.

To minimize

$$\mathcal{E}(u) := \sum_{i\in\mathcal{V}} d(f_i, u_i)^2 + \alpha \sum_{i\in\mathcal{G}\setminus\{N\}} d(u_i, u_{i+1}) + \beta \sum_{i\in\mathcal{G}\setminus\{1,N\}} d_2(u_{i-1}, u_i, u_{i+1})$$

take each summand as one φ_l in the CPPA.
Parallelization yields $c = 6$ (1D) or $c = 15$ (2D incl. mixed differences)

For the involved proximal maps we have

- $\varphi(u_i) = d(f_i, u_i)^2$: analytical solution [Ferreira, Oliveira, 2002]
- $\varphi(u_i, u_{i+1}) = d(u_i, u_{i+1})$: analytical solution [Weinmann, Storath, Demaret, 2014]
- $\varphi(u_{i-1}, u_i, u_{i+1}) = d_2(u_{i-1}, u_i, u_{i+1})$:
  - analytical solution for $\mathbb{S}^1$ [RB, Laus, Steidl, Weinmann, 2014]
  - numerical solution otherwise [Bačák, RB, Steidl, Weinmann, 2016]

Proximal Mapping of a Second Order Difference on $\mathcal{M}$

To compute

$$\operatorname{prox}_{\lambda d_2}(g) = \operatorname*{arg\,min}_{u \in \mathcal{M}^3} \left\{ \frac{1}{2} \sum_{i=1}^{3} d(u_i, g_i)^2 + \lambda d_2(u_1, u_2, u_3) \right\}$$

(sub)gradient descent method requires gradient of $d_2(x, y, z) = d(c(x, z), y)$

$$\nabla_{\mathcal{M}^3} d_2 = \left(\nabla_{\mathcal{M}} d_2(\cdot, y, z), \nabla_{\mathcal{M}} d_2(x, \cdot, z), \nabla_{\mathcal{M}} d_2(x, y, \cdot) \right)^{\mathrm{T}}.$$

For $y \neq c(x, z)$ and an ONB $\{\xi_1, \ldots, \xi_n\}$ of $T_x\mathcal{M}$

- $\nabla_{\mathcal{M}} d_2(x, \cdot, z)(y) = \dfrac{\log_y c(x, z)}{\| \log_y c(x, z) \|_y} \in T_y\mathcal{M}$
- $\nabla_{\mathcal{M}} d_2(\cdot, y, z)$ by chain rule

$$\nabla_{\mathcal{M}} d_2(\cdot, y, z)(x) = \sum_{k=1}^{n} \left\langle \frac{\log_{c(x)} y}{\| \log_{c(x)} y \|_{c(x)}}, D_x c[\xi_k] \right\rangle_{c(x)}, \quad \xi_k \in T_x\mathcal{M}.$$

Proximal Mapping of a Second Order Difference on $\mathcal{M}$

To compute

$$\operatorname{prox}_{\lambda d_2}(g) = \operatorname*{arg\,min}_{u \in \mathcal{M}^3} \left\{ \frac{1}{2} \sum_{i=1}^{3} d(u_i, g_i)^2 + \lambda d_2(u_1, u_2, u_3) \right\}$$

(sub)gradient descent method requires gradient of $d_2(x, y, z) = d(c(x, z), y)$

$$\nabla_{\mathcal{M}^3} d_2 = (\nabla_{\mathcal{M}} d_2(\cdot, y, z), \nabla_{\mathcal{M}} d_2(x, \cdot, z), \nabla_{\mathcal{M}} d_2(x, y, \cdot))^{\mathrm{T}}.$$

For $y \neq c(x, z)$ and an ONB $\{\xi_1, \dots, \xi_n\}$ of $T_x\mathcal{M}$

- $\nabla_{\mathcal{M}} d_2(x, \cdot, z)(y) = \dfrac{\log_y c(x, z)}{\|\log_y c(x, z)\|_y} \in T_y\mathcal{M}$
- $\nabla_{\mathcal{M}} d_2(\cdot, y, z)$ by chain rule

$$\nabla_{\mathcal{M}} d_2(\cdot, y, z)(x) = \sum_{k=1}^{n} \left\langle \frac{\log_{c(x)} y}{\| \log_{c(x)} y \|_{c(x)}}, D_x c[\xi_k] \right\rangle_{c(x)}, \quad \xi_k \in T_x\mathcal{M}.$$

Geodesic Variation

How do small changes in x affect the geodesic?

- $\sigma_{x,\xi_k}(s)$, $k = 1, \dots, n$, $s \in (-\varepsilon, \varepsilon)$:
  curve starting in $\sigma_{x,\xi_k}(0) = x$ with direction $\sigma'_{x,\xi_k}(0) = \xi_k$
- $\zeta_k(s)$: direction in $\sigma_{x,\xi_k}(s)$ towards z.

$\Rightarrow$ geodesic variation of the geodesic $\gamma_{\widehat{x,z}}$

$$\Gamma_k(s,t) := \exp_{\sigma_{x,\xi_k}(s)}\left(t\zeta_k(s)\right), \quad s \in (-\varepsilon, \varepsilon),\ t \in [0,T],\ T = d(x,z)$$

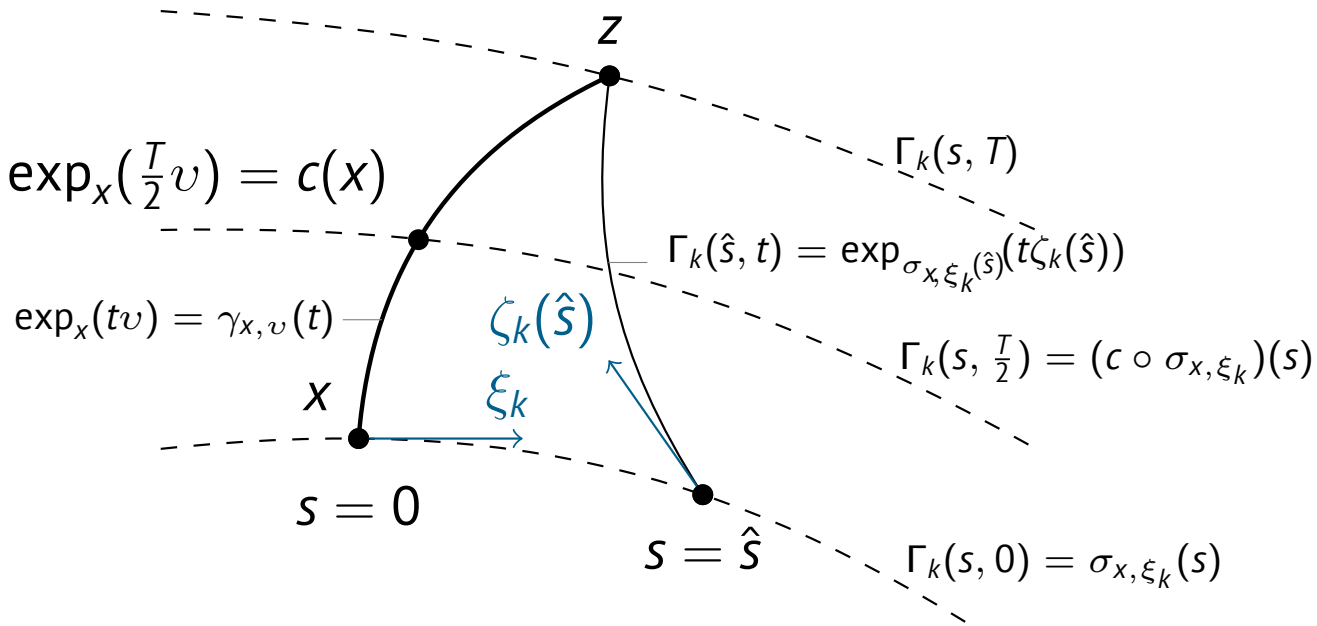

Jacobi Fields

Indicate directions of change along the geodesic and rephrase computation of the gradient to...

The Jacobi field J_k, $k = 1, \dots, n$, along $\gamma_{\widehat{x,z}}$ is defined by

$$J_k(t) := \frac{\partial}{\partial s}\Gamma_k(s,t)\big|_{s=0}, \quad t \in [0,T]$$

Lemma

$$D_x c[\xi_k] = J_k\left(\tfrac{T}{2}\right)$$

Lemma

A Jacobi field J_k fulfills the System of ODEs

$$\frac{D^2}{\mathrm{d}t^2}J_k + R(J_k, \dot\gamma_{\widehat{x,z}})\dot\gamma_{\widehat{x,z}} = 0, \qquad J_k(0) = \xi_k,\ J_k(T) = 0$$

with the Riemannian curvature tensor $R\colon T\mathcal{M} \times T\mathcal{M} \times T\mathcal{M} \to T\mathcal{M}$.

Riemannian Symmetric Spaces

At least in beautiful Spaces we can solve the system of ODEs

- For every $x \in \mathcal{M}$ exists an isometry s_x on $\mathcal{M}$, i.e.

$$s_x(x) = x, D_x s[\xi] = -\xi, \qquad \text{for all } \xi \in T_x\mathcal{M}$$

- covariant derivative

$$\nabla R = 0$$

$\Rightarrow$ the system of ODEs simplifies to a a linear system of ODEs with constant coefficients

- Examples of symmetric spaces
  - Spheres $\mathbb{S}^n$
  - Hyperbolic Spaces
  - positive definite matrices $\mathcal{P}(s)$
  - Grasmannians

Riemannian symmetric spaces are the most beautiful and most important Riemannian manifolds.

[Eschenburg, 1997]

The Derivative $D_x c[\xi_k]$ in Symmetric Spaces

Finally we are able to evaluate the Jacobi field at the mid point $T/2$

Given a specific ONB $\{\xi_1, \dots, \xi_n\}$ at $t = 0$ and its parallel transport $\{\Theta_1(t), \dots, \Theta_n(t)\}$ along the geodesic, i.e.

$$J_k(t) = \sum_{i=1}^{n} a_{k,i}(t)\Theta_i(t).$$

Corollary

With $T = d(x, z)$and κ_i "characterize curvature" we have for $k = 1, \dots, n$

$$D_x c[\xi_k] = J_k\left(\tfrac{T}{2}\right) = \begin{cases} \dfrac{\sinh\left(\sqrt{-\kappa_k}\frac{T}{2}\right)}{\sinh(\sqrt{-\kappa_k}T)}\Theta_k(\tfrac{T}{2}), & \text{if } \kappa_k < 0, \\ \dfrac{\sin\left(\sqrt{\kappa_k}\frac{T}{2}\right)}{\sin(\sqrt{\kappa_k}T)}\Theta_k(\tfrac{T}{2}), & \text{if } \kappa_k > 0, \\ \frac{1}{2}\Theta_k(\tfrac{T}{2}), & \text{if } \kappa_k = 0. \end{cases}$$

$\Rightarrow$ Gradient descent to approximate the $\operatorname{prox}_{\lambda d_2}$ on $\mathcal{M}^3$.

A Signal of Cyclic Data

Denoising a phase valued signal.

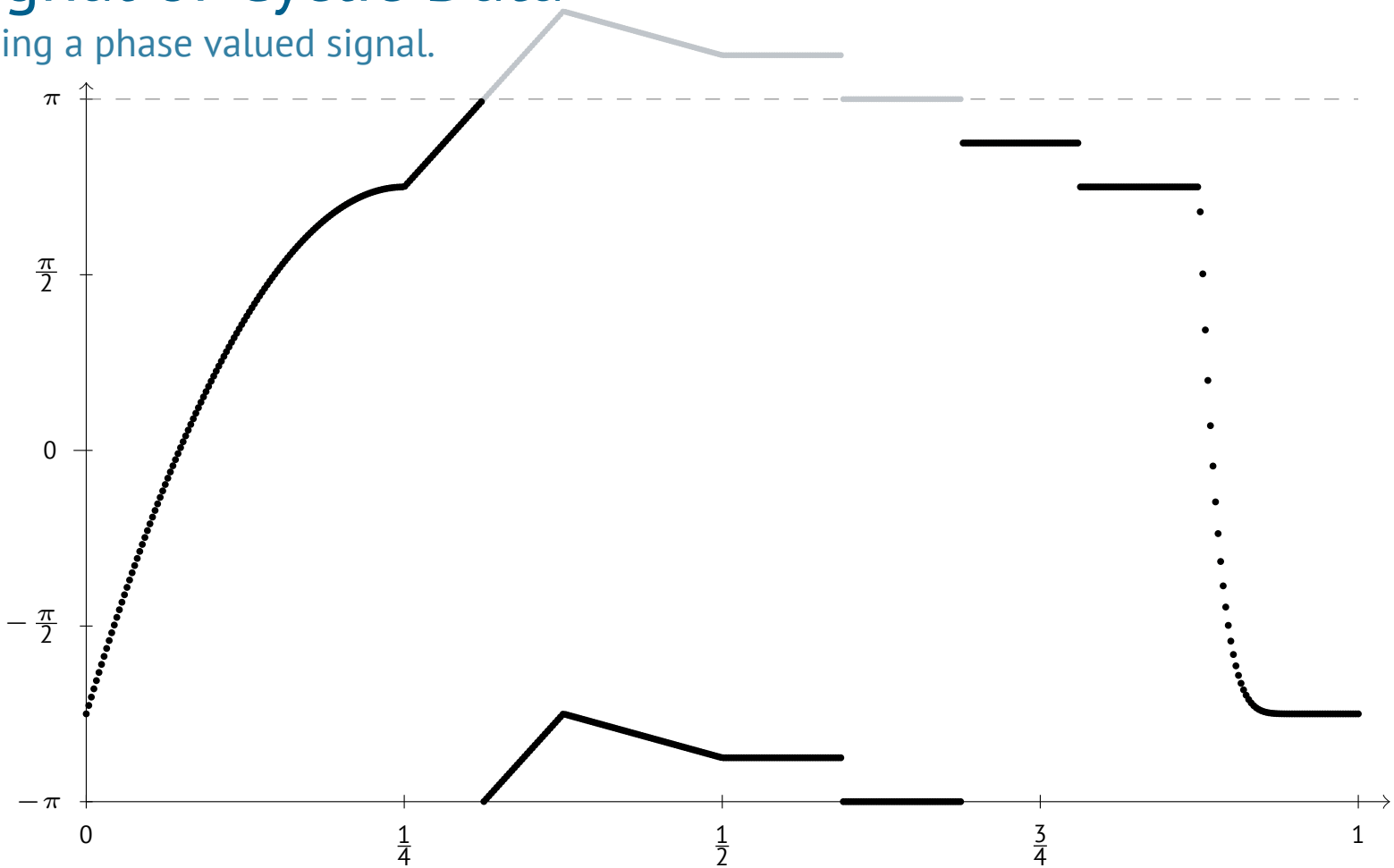

- function $f\colon [0,1] \to \mathbb{S}^1$ sampled to obtain data $f_0 = (f_{0,i})_{i=1}^{500}$
- f could be a wrapped version of the gray plot, hence
- jumps $> \pi$ at $\frac{5}{16}$ and $\frac{11}{16}$ are due to the representation system

A Signal of Cyclic Data

Denoising a phase valued signal.

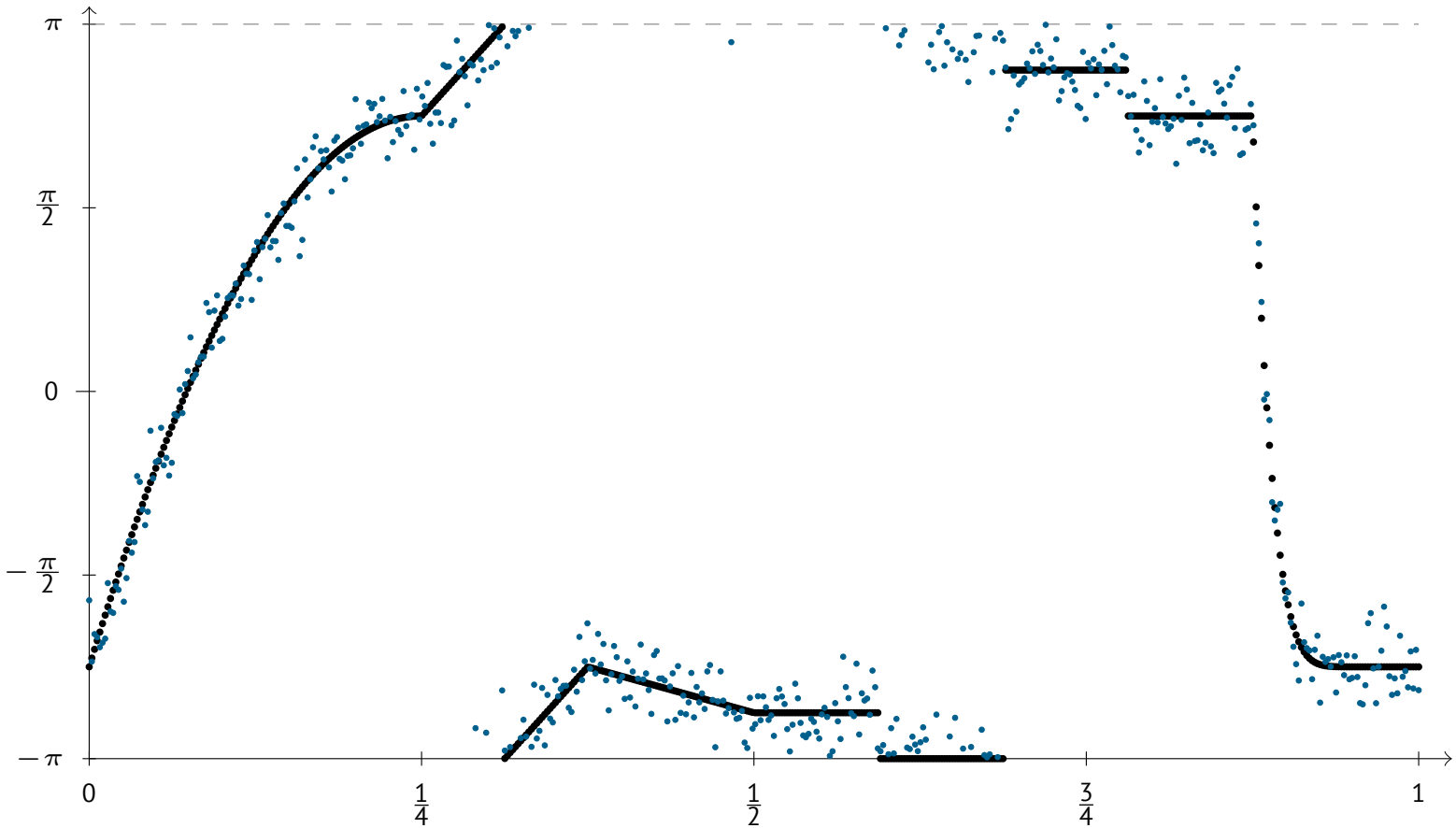

- function $f\colon [0,1] \to \mathbb{S}^1$ sampled to obtain data $f_0 = (f_{0,i})_{i=1}^{500}$
- adding wrapped Gaussian noise, $\sigma = 0.2$
- noisy data $f_n = (f_0 + \eta)_{2\pi}$

A Signal of Cyclic Data

Denoising a phase valued signal.

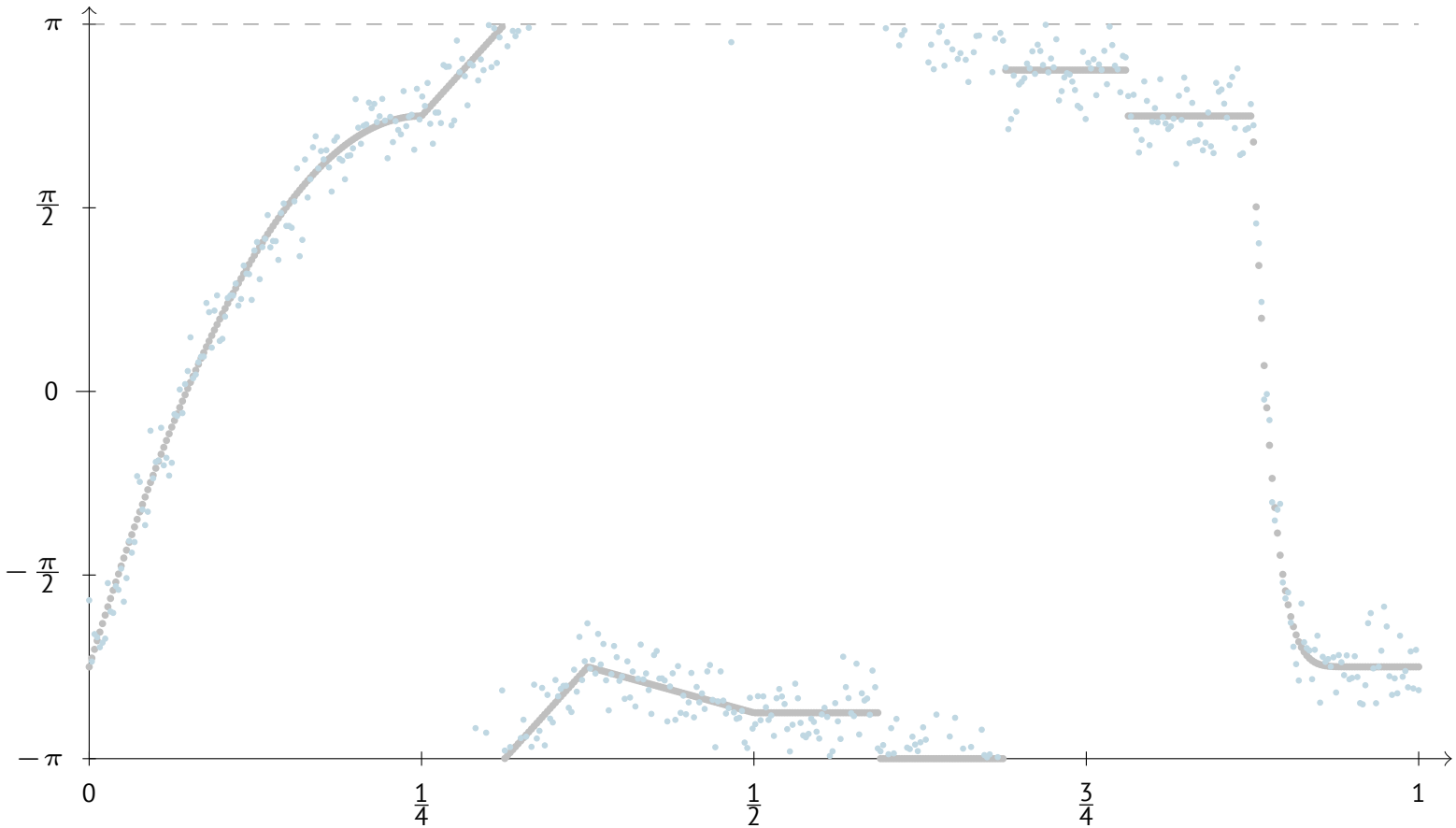

- comparison of f_o & f_n with

A Signal of Cyclic Data

Denoising a phase valued signal.

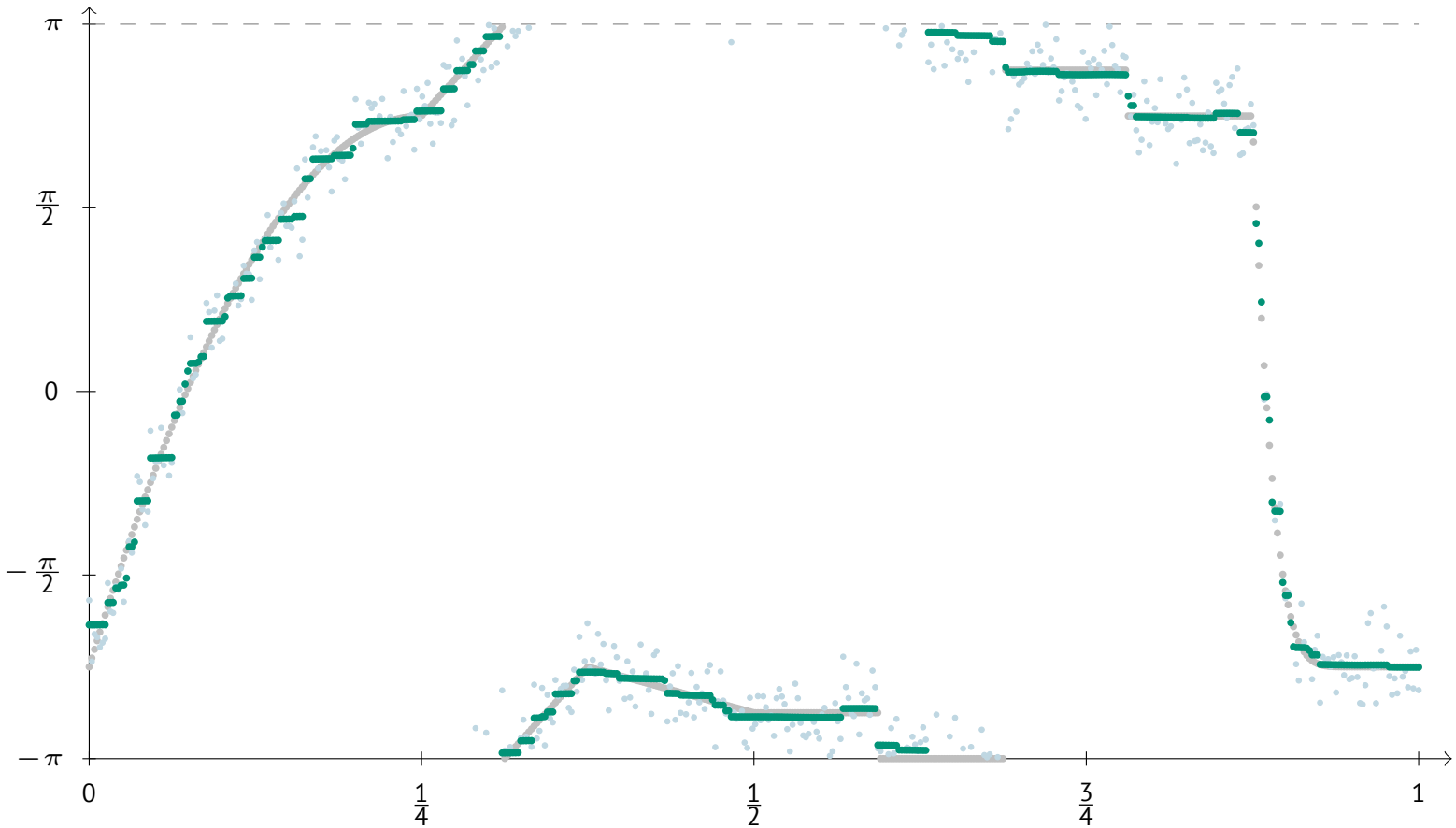

- comparison of f_0 & f_n with f_1
- denoising TV_1 ($\alpha = \frac{3}{4}$, $\beta = 0$)
- but: stair casing

A Signal of Cyclic Data

Denoising a phase valued signal.

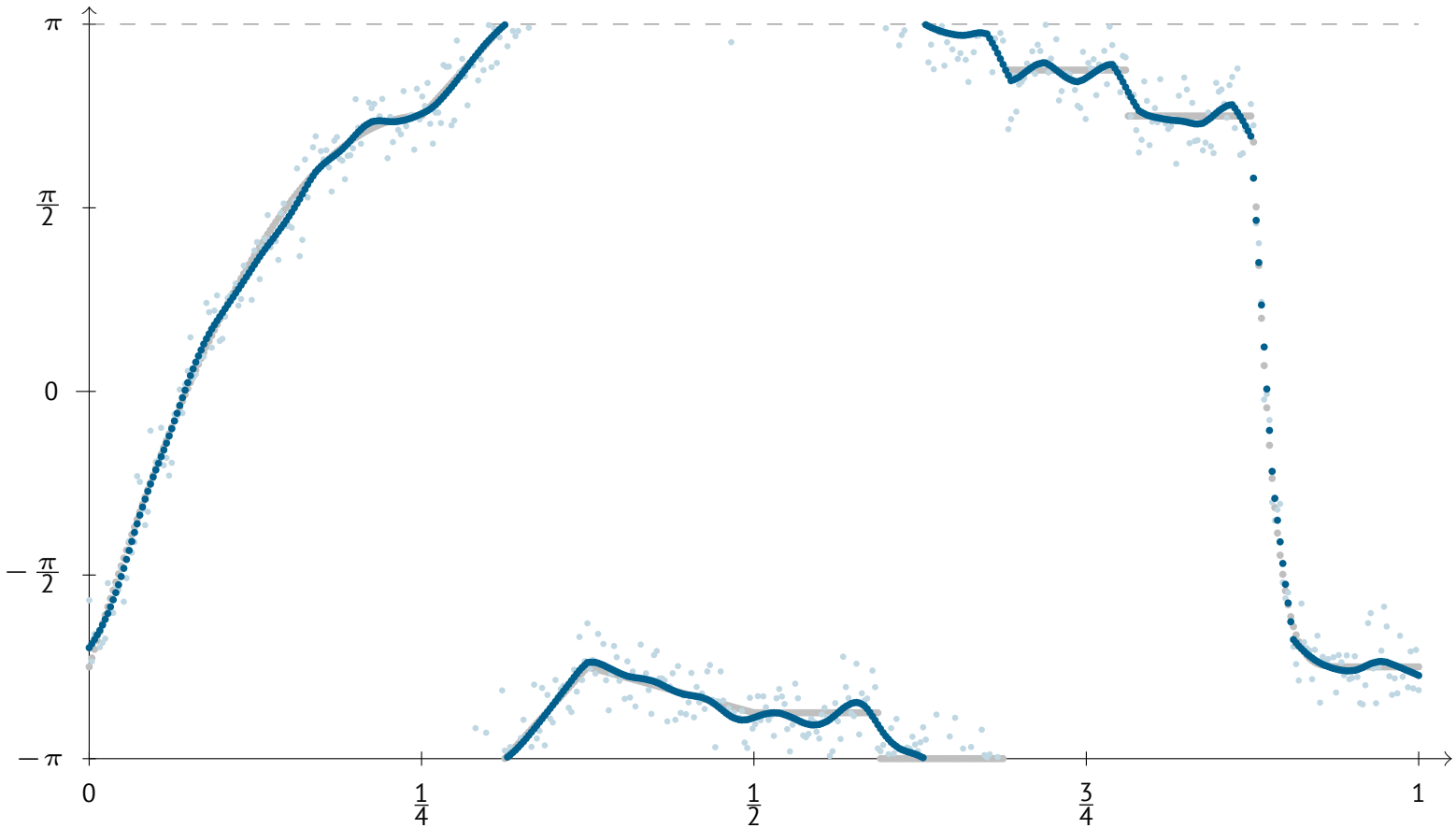

- comparison of f_o & f_n with f_2
- denoising TV_2 ($\alpha = 0, \beta = \frac{3}{2}$)
- but: no plateaus

A Signal of Cyclic Data

Denoising a phase valued signal.

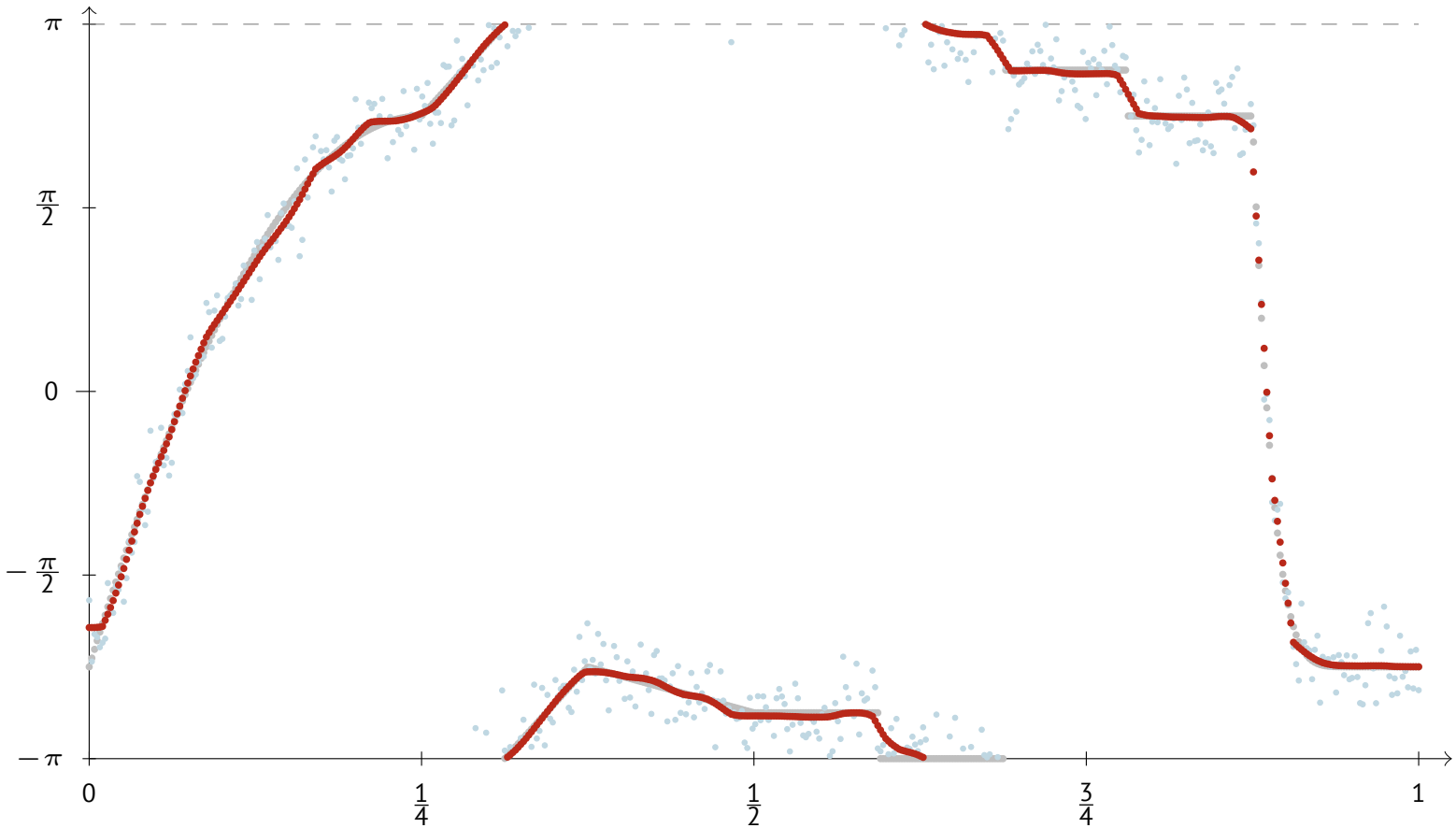

- comparison of f_0 & f_n with f_3
- denoising TV_1 & TV_2 ($\alpha = \frac{1}{2}$, $\beta = 1$)
- smallest mean squared error

Bernoulli's Lemniscate on the Sphere $\mathbb{S}^2$

$$\gamma(t) := \frac{a\sqrt{2}}{\sin^2(t)+1}\left(\cos(t), \cos(t)\sin(t)\right)^{\mathrm{T}}, \quad t \in [0, 2\pi], a = \frac{\pi}{2\sqrt{2}}.$$

Generate a sphere-valued signal by putting it into the tangential plane of the north pole

$$\gamma_S(t) = \log_p(\gamma(t)), p = (0,0,1)^{\mathrm{T}}$$

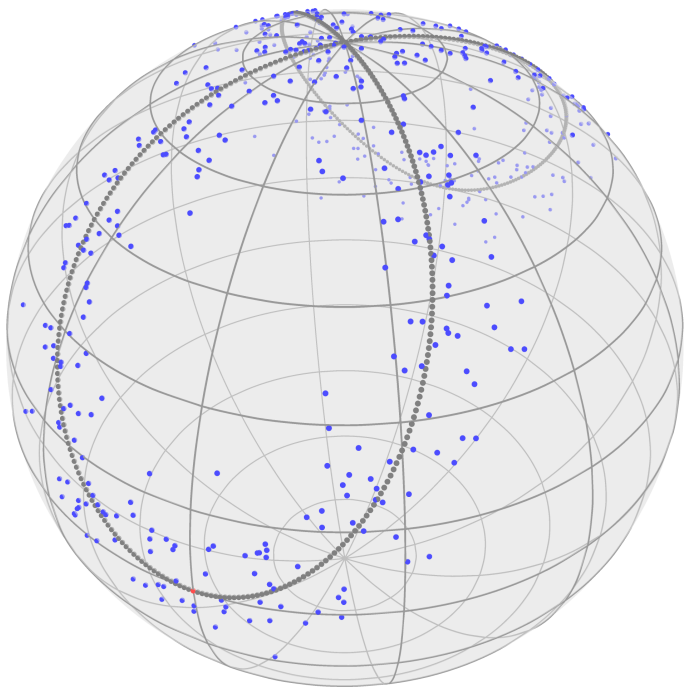

noisy lemniscate of Bernoulli on $\mathbb{S}^2$, Gaussian noise, $\sigma = \frac{\pi}{30}$, on $T_p\mathbb{S}^2$.

Bernoulli's Lemniscate on the Sphere $\mathbb{S}^2$

$$\gamma(t) := \frac{a\sqrt{2}}{\sin^2(t)+1}\left(\cos(t), \cos(t)\sin(t)\right)^{\mathrm{T}}, \quad t \in [0, 2\pi], a = \frac{\pi}{2\sqrt{2}}.$$

Generate a sphere-valued signal by putting it into the tangential plane of the north pole

$$\gamma_S(t) = \log_p(\gamma(t)), p = (0,0,1)^{\mathrm{T}}$$

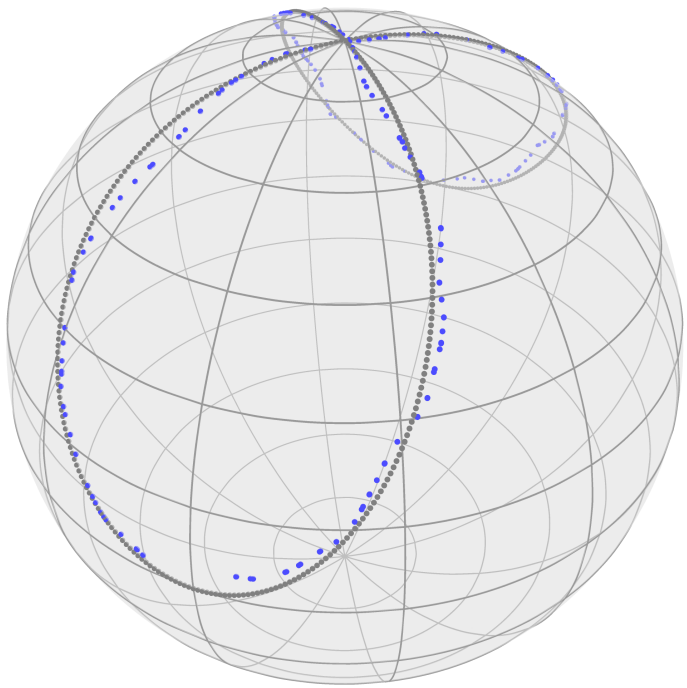

reconstruction with TV_1, $\alpha = 0.21$, $\mathrm{MAE} = 4.08 \times 10^{-2}$.

Bernoulli's Lemniscate on the Sphere $\mathbb{S}^2$

$$\gamma(t) := \frac{a\sqrt{2}}{\sin^2(t)+1}\left(\cos(t), \cos(t)\sin(t)\right)^{\mathrm{T}}, \quad t \in [0, 2\pi], a = \frac{\pi}{2\sqrt{2}}.$$

Generate a sphere-valued signal by putting it into the tangential plane of the north pole

$$\gamma_S(t) = \log_p(\gamma(t)), p = (0,0,1)^{\mathrm{T}}$$

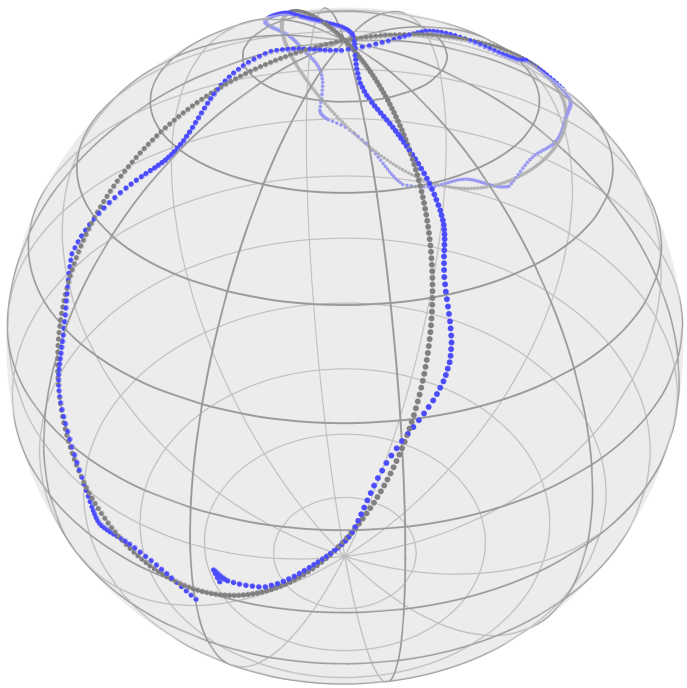

reconstruction with TV_2, $\alpha = 0$, $\beta = 10$, $\mathrm{MAE} = 3.66 \times 10^{-2}$.

Bernoulli's Lemniscate on the Sphere $\mathbb{S}^2$

$$\gamma(t) := \frac{a\sqrt{2}}{\sin^2(t)+1}\left(\cos(t), \cos(t)\sin(t)\right)^{\mathrm{T}}, \quad t \in [0, 2\pi], a = \frac{\pi}{2\sqrt{2}}.$$

Generate a sphere-valued signal by putting it into the tangential plane of the north pole

$$\gamma_S(t) = \log_p(\gamma(t)), p = (0,0,1)^{\mathrm{T}}$$

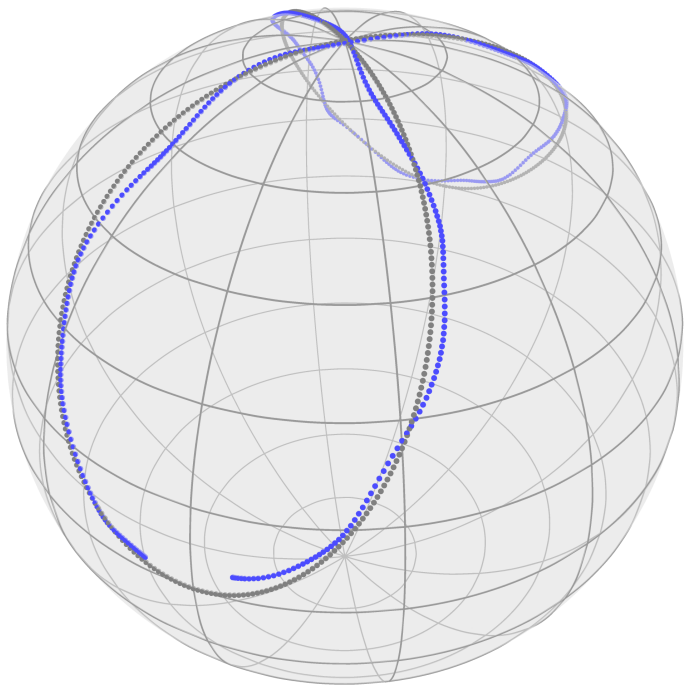

reconstruction with TV_1 & TV_2, $\alpha = 0.16$, $\beta = 12.4$, $\mathrm{MAE} = 3.27 \times 10^{-2}$.

Inpainting of $\mathcal{P}(3)$-valued Images

Illustrate symmetric positive definite 3×3 matrices as ellipsoids

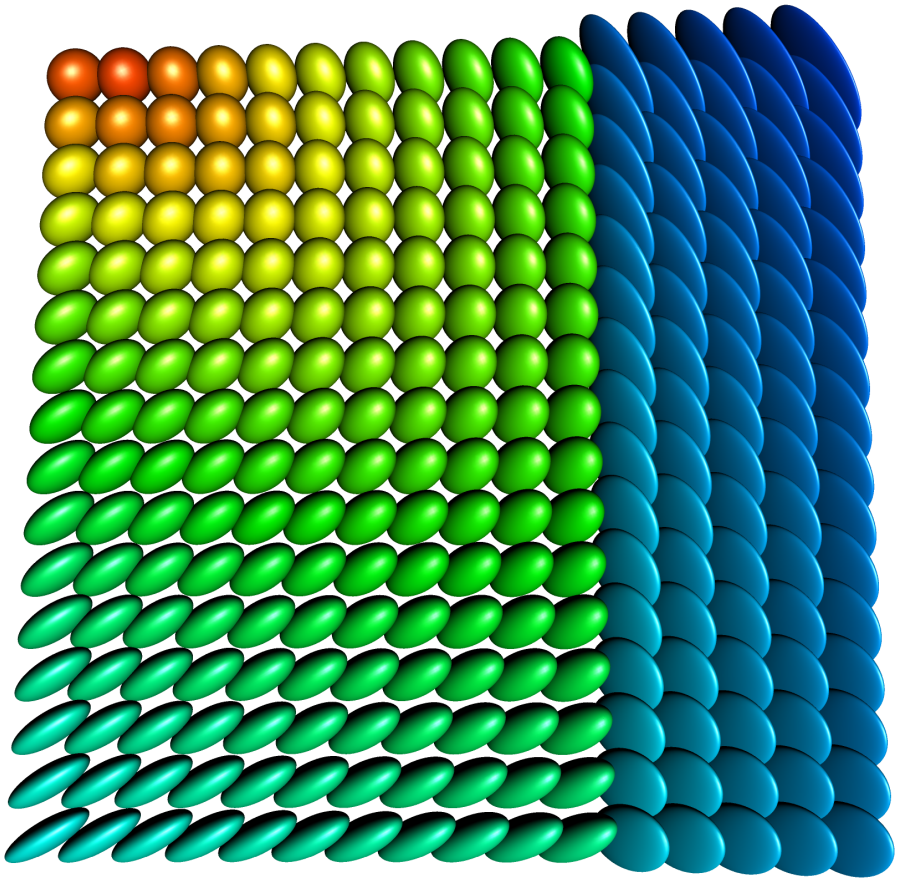

original data

Inpainting of $\mathcal{P}(3)$-valued Images

Illustrate symmetric positive definite 3×3 matrices as ellipsoids

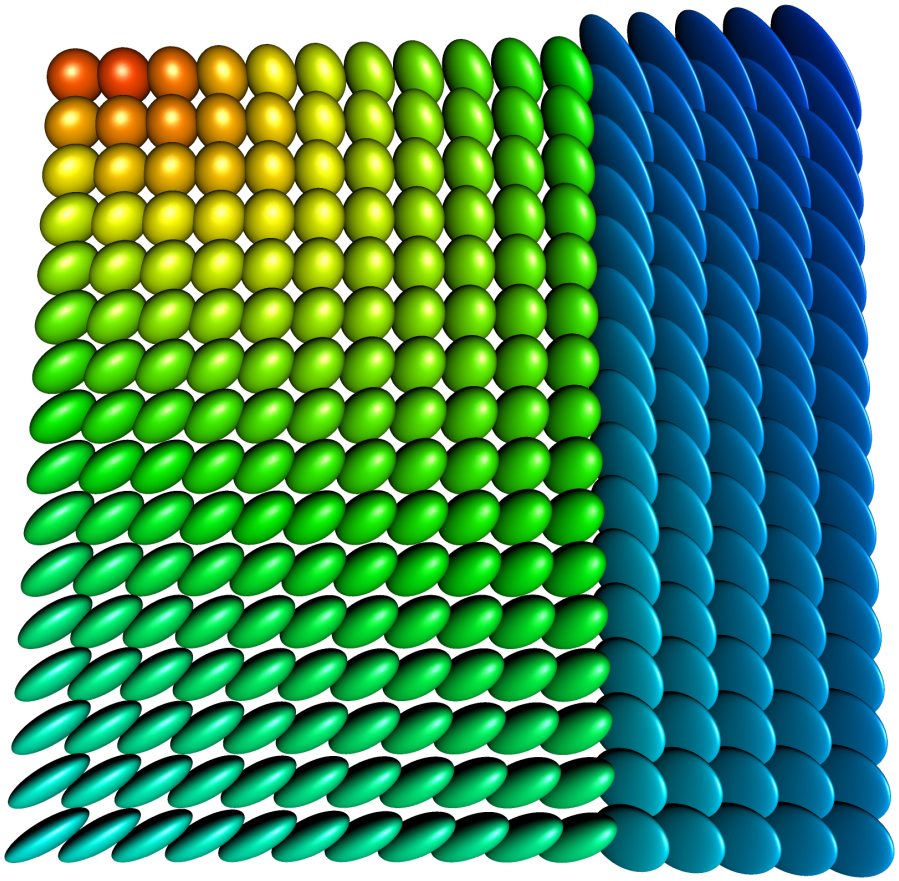

original data

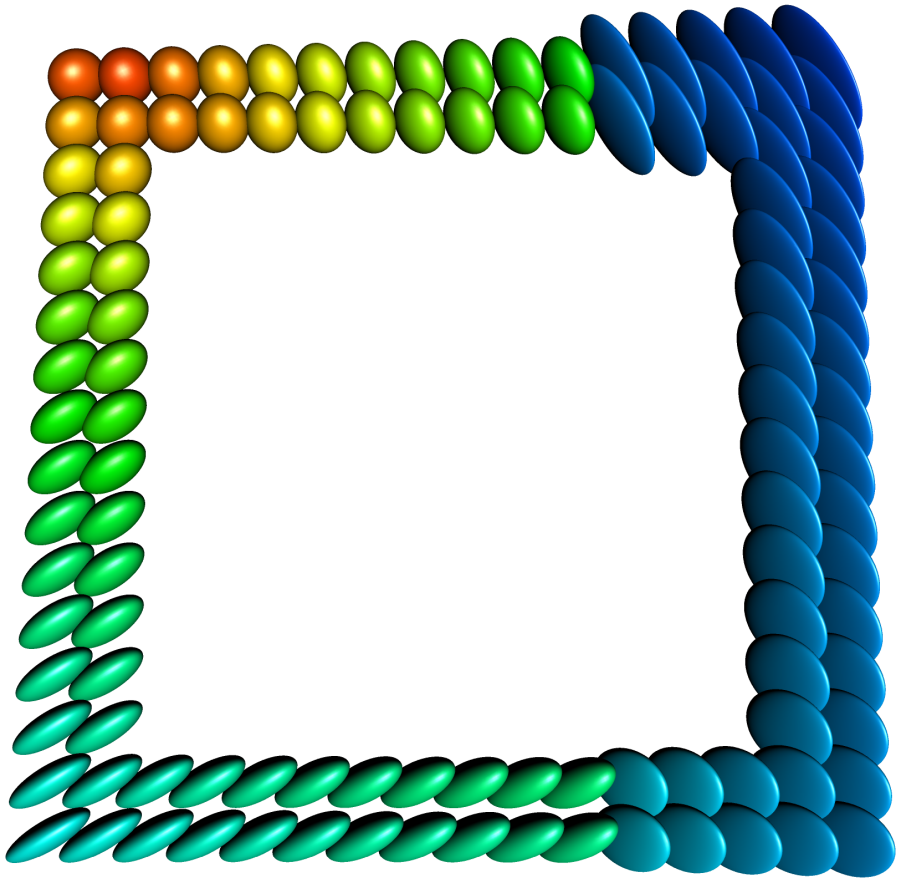

lost (a lot of) data

Inpainting of $\mathcal{P}(3)$-valued Images

Illustrate symmetric positive definite 3×3 matrices as ellipsoids

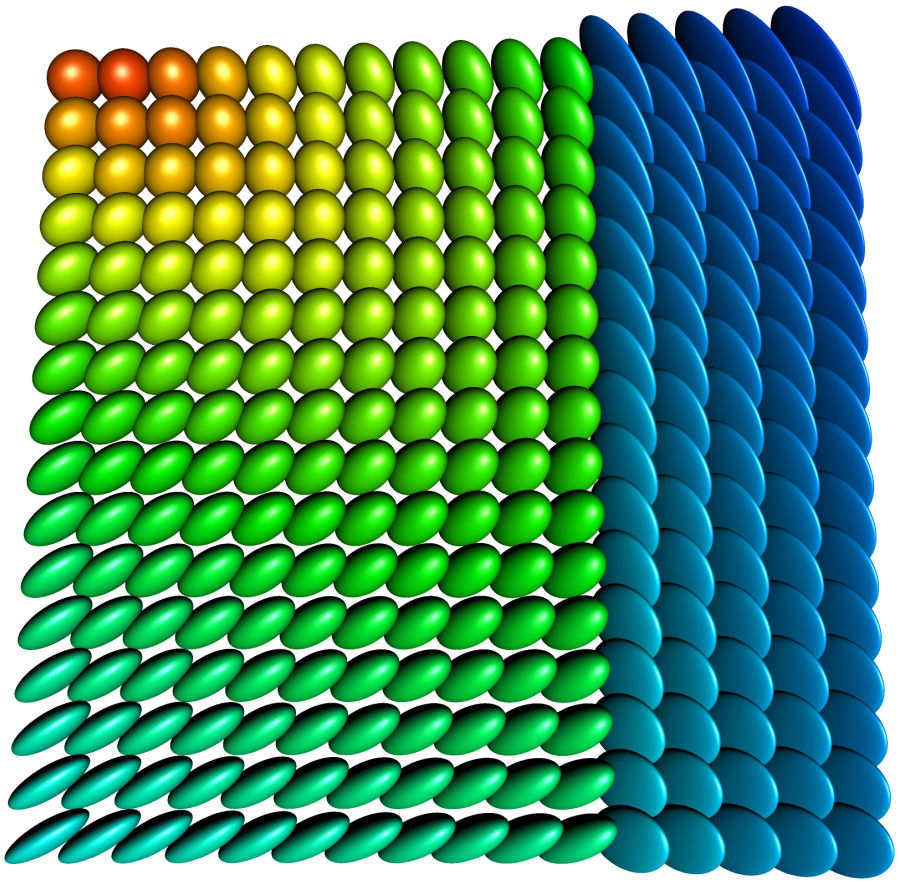

original data

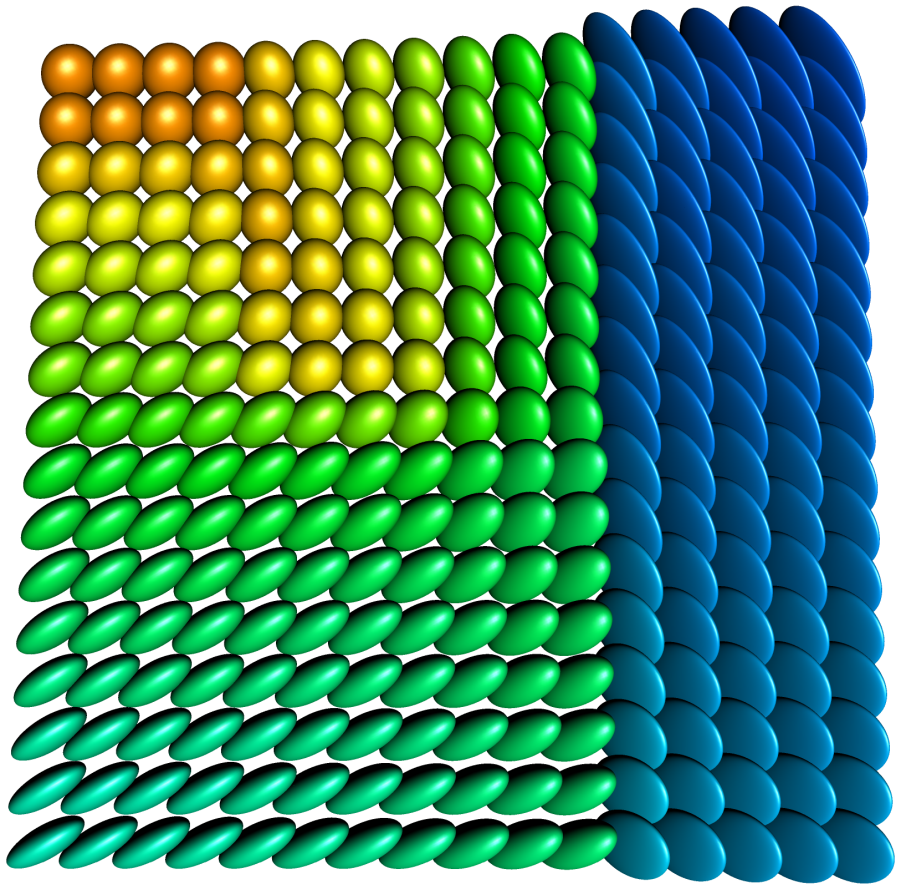

inpainted with $\alpha = \beta = 0.05$,
MAE $= 0.0929$

Inpainting of $\mathcal{P}(3)$-valued Images

Illustrate symmetric positive definite 3×3 matrices as ellipsoids

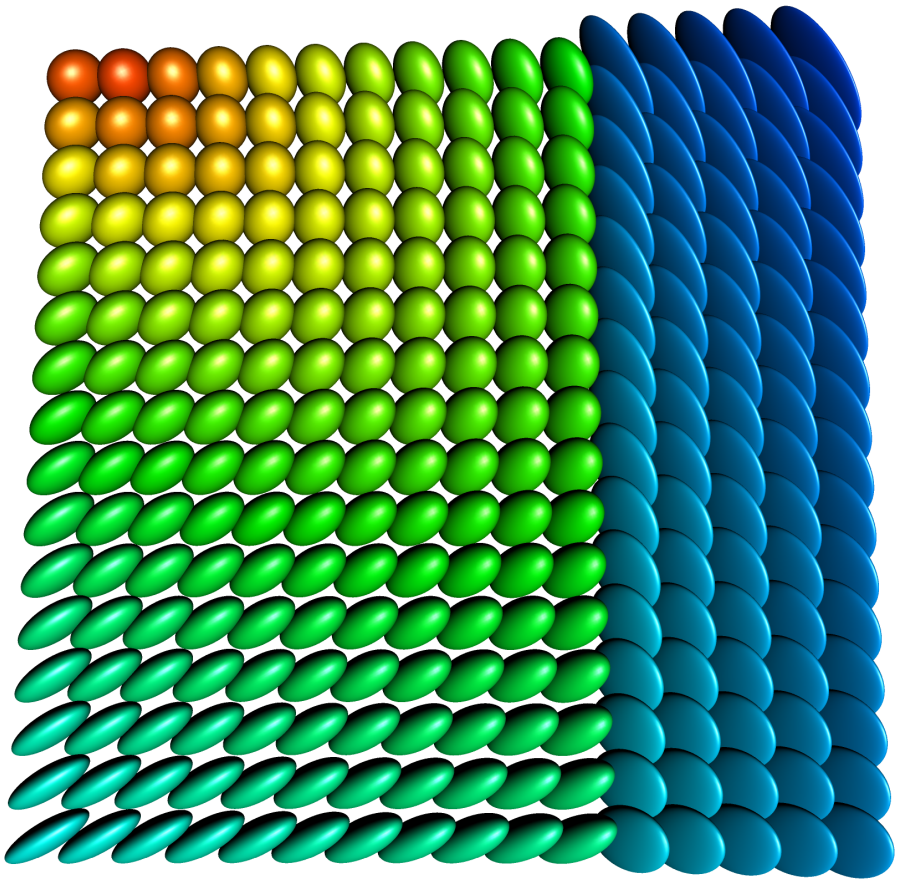

original data

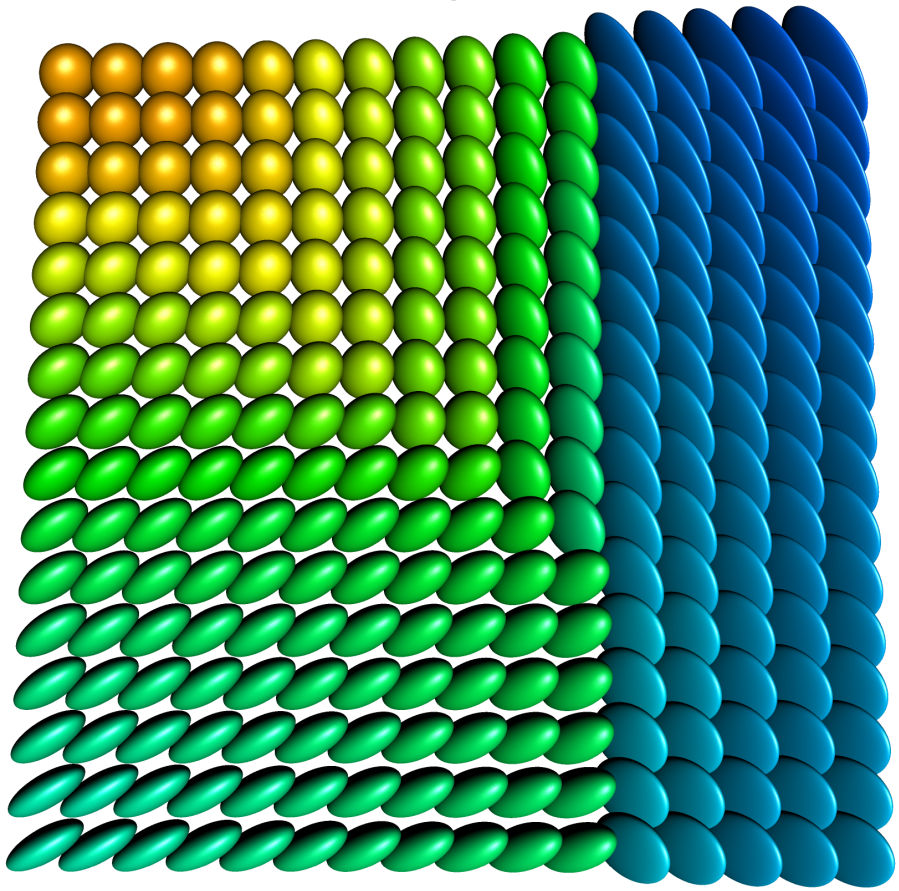

inpainted with $\alpha = 0.1$,
MAE $= 0.0712$

Diffusion Tensor Magnetic Resonance Imaging

Dataset $\mathcal{P}(3)^{112\times112\times50}$ of the human head, traversal plane $z = 28$

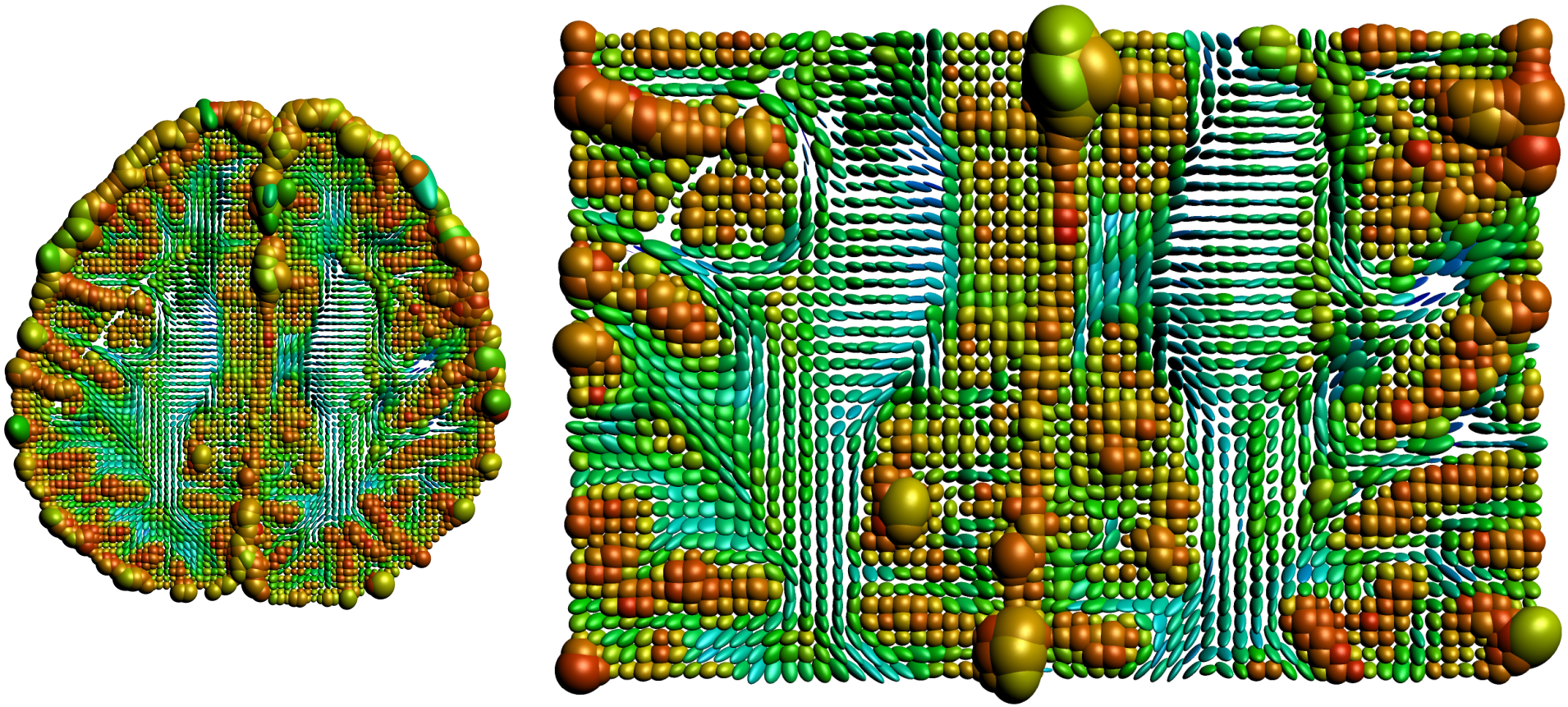

Original Data

(Data available from The Camino Project, cmic.cs.ucl.ac.uk/camino)

Diffusion Tensor Magnetic Resonance Imaging

Dataset $\mathcal{P}(3)^{112\times112\times50}$ of the human head, traversal plane $z = 28$

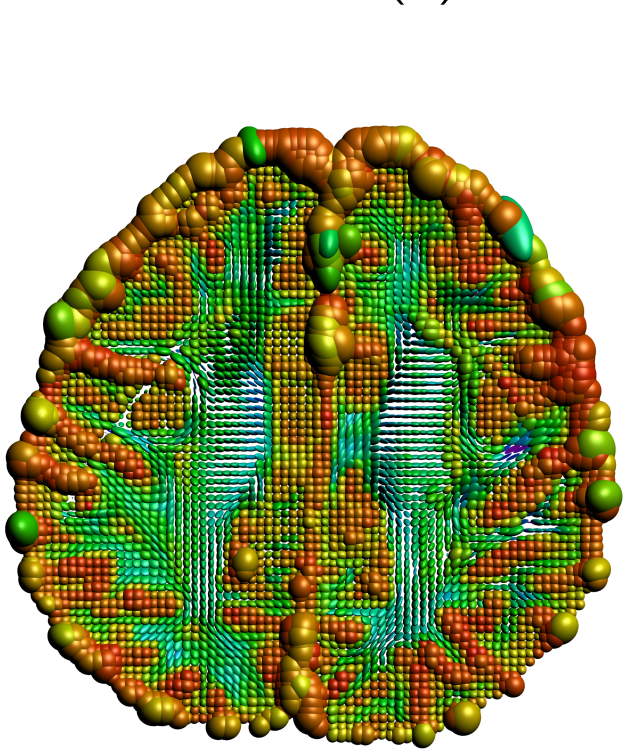

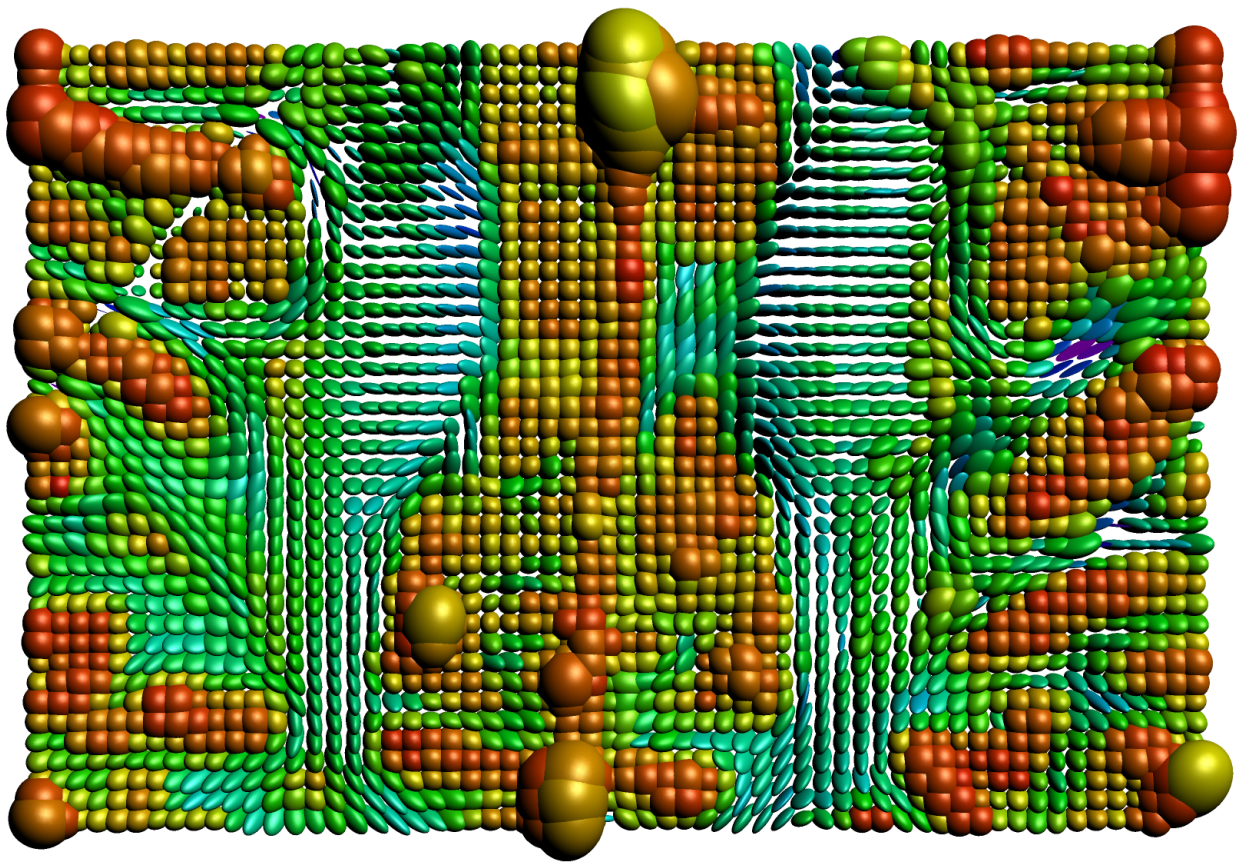

TV-denoised, $\alpha = 0.1$

(Data available from The Camino Project, cmic.cs.ucl.ac.uk/camino)

Diffusion Tensor Magnetic Resonance Imaging

Dataset $\mathcal{P}(3)^{112\times112\times50}$ of the human head, traversal plane $z = 28$

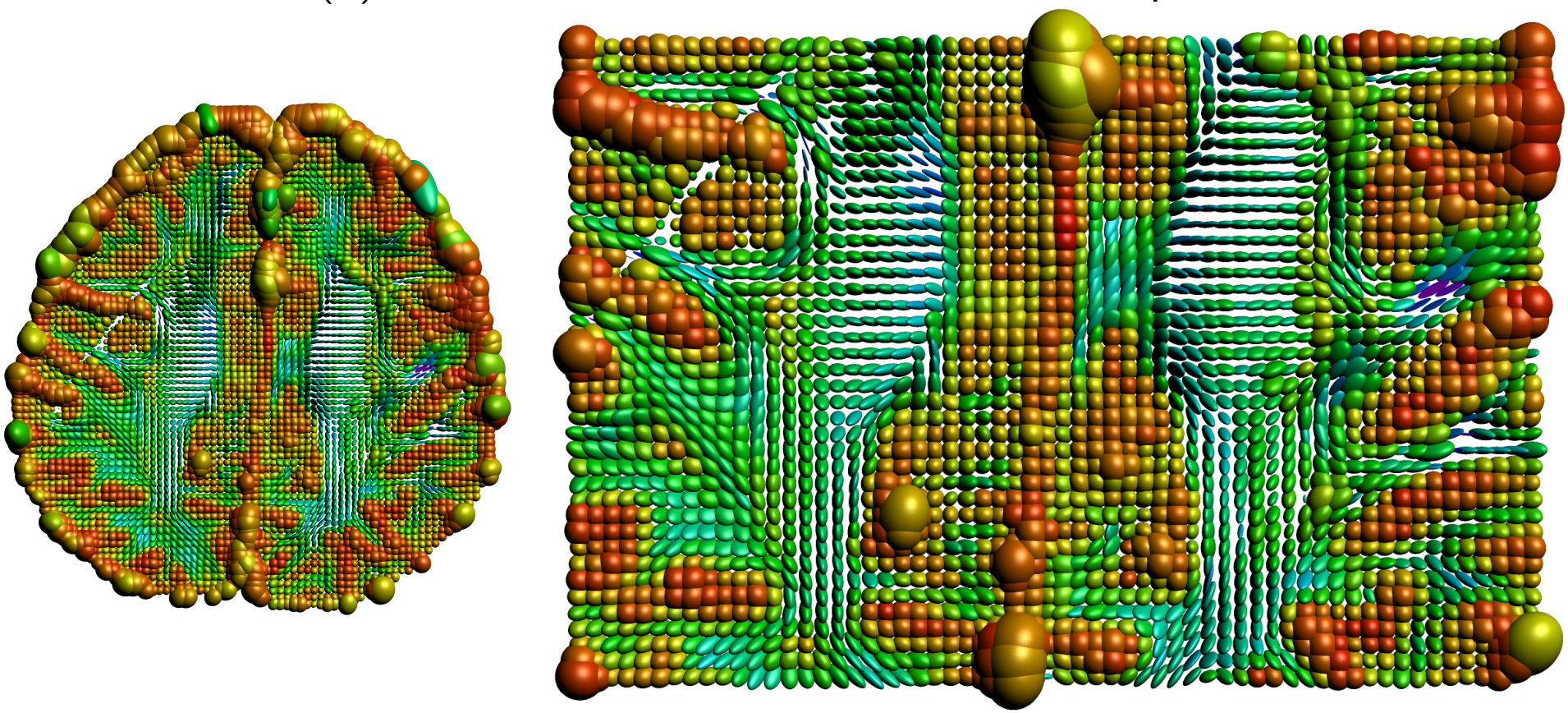

TV&TV2-denoised, $\alpha = 0.05, \beta = 0.1$

(Data available from The Camino Project, cmic.cs.ucl.ac.uk/camino)

Conclusion

We have for manifold valued images $f\colon \mathcal{V} \to \mathcal{M}$

- a model for a first and second order TV-type functional $\mathcal{E}(u)$
- cyclic proximal point algorithm to minimize $\mathcal{E}(u)$
- computed the proximal mappings using Jacobi fields
- proof of convergence
- Code available:

  http://www.mathematik.uni-kl.de/imagepro/members/bergmann/mvirt/

Conclusion

We have for manifold valued images $f\colon \mathcal{V} \to \mathcal{M}$

- a model for a first and second order TV-type functional $\mathcal{E}(u)$
- cyclic proximal point algorithm to minimize $\mathcal{E}(u)$
- computed the proximal mappings using Jacobi fields
- proof of convergence
- Code available:

  http://www.mathematik.uni-kl.de/imagepro/members/bergmann/mvirt/

What's next?

For manifold-valued TV

- relax to Half-Quadratic Minimization [RB, Chan, Hielscher, Persch, Steidl, 2016]
- faster algorithm: Parallel Douglas-Rachford (J. Persch, CP2, 5:10pm)

Future work

- an isotropic second order TV, other couplings, algorithms, manifolds,...
- other image processing tasks for manifold-valued images

Literature

[1] M. Bačák, RB, G. Steidl, and A. Weinmann. A second order non-smooth variational model for restoring manifold-valued images. *SIAM J. Sci. Comput.*, 2016.

[2] RB, F. Laus, G. Steidl, and A. Weinmann. Second order differences of cyclic data and applications in variational denoising. *SIAM J. Imaging Sci.*, 2014.

[3] RB and A. Weinmann. A second order TV-type approach for inpainting and denoising higher dimensional combined cyclic and vector space data. *JMIV*, 2016.

[4] RB, R. H. Chan, R. Hielscher, J. Persch, and G. Steidl. Restoration of manifold-valued images by half-quadratic minimization. *Inverse Problems and Imaging*, 2016.

[5] RB, J. Persch, and G. Steidl. A parallel Douglas-Rachford algorithm for restoring images with values in symmetric Hadamard manifolds. *SIAM J. Imaging Sci.*, 2015, accepted.

Literature

[1] M. Bačák, RB, G. Steidl, and A. Weinmann. A second order non-smooth variational model for restoring manifold-valued images. *SIAM J. Sci. Comput.*, 2016.

[2] RB, F. Laus, G. Steidl, and A. Weinmann. Second order differences of cyclic data and applications in variational denoising. *SIAM J. Imaging Sci.*, 2014.

[3] RB and A. Weinmann. A second order TV-type approach for inpainting and denoising higher dimensional combined cyclic and vector space data. *JMIV*, 2016.

[4] RB, R. H. Chan, R. Hielscher, J. Persch, and G. Steidl. Restoration of manifold-valued images by half-quadratic minimization. *Inverse Problems and Imaging*, 2016.

[5] RB, J. Persch, and G. Steidl. A parallel Douglas-Rachford algorithm for restoring images with values in symmetric Hadamard manifolds. *SIAM J. Imaging Sci.*, 2015, accepted.

Thank you for your attention.